Design of a PCB integrated eddy current sensor with shield feature for radial rotor displacement measurement

Dominik WIMMER, Markus HUTTERER, Manfred SCHRÖDL

TU Wien, Institute of Energy Systems and Electrical Drives, Gußhausstraße 25-29, 1040 Vienna, Austria, dominik.wimmer@tuwien.ac.at

Abstract

Active magnetic bearings require position feedback to enable a stable control of a levitating rotor. The position information can be provided by explicit position sensors or the usage of self-sensing bearing topologies. In this study an investigation of a PCB integrated eddy current sensor for radial rotor displacement measurement is conducted. In many AMB applications a short rotor length is desired to handle flexible rotor characteristics at high rotational speeds. Therefore, the active magnetic bearings, the motor as well as the sensors shall obtain a small axial length. Conventional eddy current displacement sensors often obtain a cylindrical shape with a circular measurement spot on the rotor target material, which defines the minimum axial length of the sensor arrangement. The aim of this study is to design a low-cost PCB integrated eddy current sensor with an arc-shaped measurement spot and low axial dimension. In contrast to previous studies in this field, it is investigated if it is possible to achieve a feasible sensor design without the use of a coupled coil arrangement of excitation- and sense coils. This study covers the sensor design, measurements on a prototype as well as a performance comparison between a non-shielded and a shielded sensor design.

Keywords: AMB sensor, radial displacement measurement, eddy current sensor

1. Introduction

Active magnetic bearings (AMBs) are often used for contact-free rotor suspension where conventional rolling bearings are not able to meet the increasing demands of high-speed applications. The control loop of AMBs requires feedback of the rotor position to enable a stable control. The rotor position can be obtained by sensor-based or self-sensing approaches. Self-sensing approaches (Maslen 2006) are a very exclusive way to determine the rotor position but the methods are mostly very specific for a certain magnetic arrangement and cannot be easily transferred to other AMB topologies. In contrast, AMB sensors require additional construction space, which can increase the size and weight of an AMB system. Especially, a longer shaft can cause problems by higher thermal expansion in the axial direction and lower natural frequencies of flexible rotor characteristics. In contrast to inductive sensor designs, also eddy current sensors are well established for position measurement but do not have special requirements concerning the magnetic properties of the target material. Special applications like AMBs often require adapted sensor designs to fulfill demands concerning sensor integration, measurement range, bandwidth, linearity, noise and of course the cost factor. Previous eddy current sensor designs for radial rotor displacement measurements deal with widely concentrated windings (Štusák 2014, Wang et al. 2018) or with a coupled coil arrangement of excitation and measurement coils (Larsonneur & Bühler 2004, Grobler et al. 2017). This study covers the design of a PCB integrated sensor design with low axial dimension and an integral (non-concentrated) measurement over the rotor surface. Furthermore, a very close coupling between the sensor coils and the rotor is aspired to delimit the stray field area to a minimum to reduce the impact of a desired sensor shield cage.

The principle of eddy current sensors relies on flux expulsion in the target material, which can be mathematically described by the diffusion equation (Markovic & Perriard 2009). As a result, the penetration depth δ of alternating

magnetic flux (exponential decay) is given by

$$\delta = \sqrt{\frac{2}{\mu\gamma\omega}}\,, \tag{1}$$

with the permeability μ, the conductivity γ and the angular frequency ω. The eddy currents in the target material influence the magnetic flux distribution of a coil with alternating excitation. Thus, the presence of a conductive material can be detected by the electrical coil quantities, which enables the use for sensor applications.

2. Sensor Design

Figure 1 shows an illustration of the aspired PCB integrated sensor design for two-axis displacement measurement. The sensor arrangement consists of a sandwich with a coil-PCB in the center which is surrounded by shield-PCBs. The coil-PCB contains two opposing sense coils for each degree of freedom (x, y). Therefore, the sense coil is realized as an air coil, which is wound between multiple layers of the coil-PCB. The coil-PCB is surrounding by shield-PCBs in order to achieve a suppression of unwanted EMI couplings of close-by bearing and motor coils. Furthermore, the sensor shield provides a well-defined boundary for the stray flux of the sense coils and suppresses an undesired influence of close proximity conductive or ferromagnetic elements.

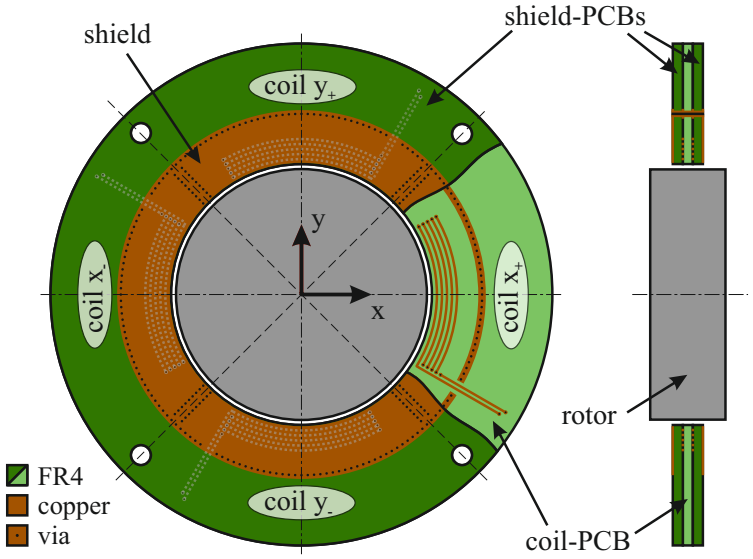

Figure 1: PCB integrated radial eddy current sensor design with optional shield-PCBs.

Table 1: Sensor design specification overview

Symbol	Parameter	Value
z_S	Axial sensor length (non-shielded design)	1.6 mm
$z_{S,shield}$	Axial sensor length (shielded design)	4.8 mm
$d_{S,o}$	Outer sensor diameter	100 mm
$d_{S,i}$	Inner sensor diameter	51.5 mm
d_R	Rotor diameter, rotor material: AW-6082	50 mm
Δx_S,Δy_S	Sensor range	±750 µm
Δx_R,Δy_R	Rotor displacement operational range	±400 µm
N	Turns per coil	16
$f_{carrier}$	Coil carrier frequency	1 MHz
$f_{-3\mathrm{dB}}$	Sensor circuit bandwidth	22 kHz

3. Sensor Prototype

Figure 2 shows the sensor prototype, which meets the design specifications according to Table 1. The admissible sensor range is designed for radial rotor displacements of $\pm 400\,\mu m$. For safety reasons, $350\,\mu m$ additional air-gap was considered to avoid a rotor-sensor collision in touch down scenarios with a safety bearing. The sense coils were implemented in a 4 layer PCB with nested windings. The nested arrangement of the windings allows the integration of 16 windings within only $2\,mm$ radial space consumption. For this reason, it

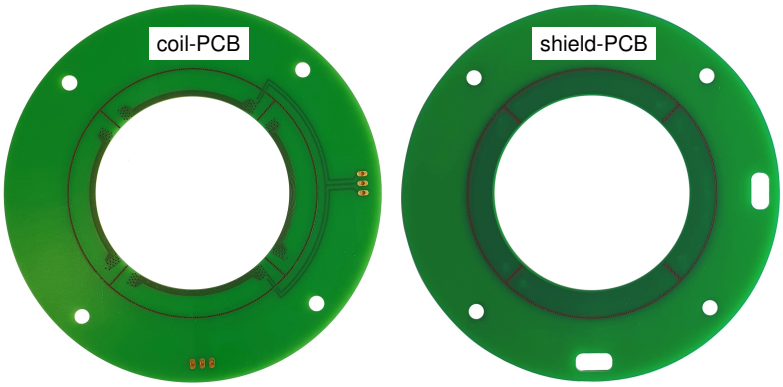

Figure 2: 4 layer coil-PCB prototype with optional 2 layer shield-PCB.

is ensured that even the outer windings are in close proximity to the target material. For achieving a shielding of the sense coils, the shield-PCBs can be stacked to the coil-PCB. Thus, the sense coils are surrounded by three-dimensional conductive chambers, which exhibit just one open side in direction of the measurement target.

4. Impedance measurements

For obtaining a deeper insight into the frequency-dependent characteristic of the sense coil, the impedance was determined for selected coil-rotor distances (Fig. 3). It can be seen that the sense coil has an ohmic-inductive behavior in the depicted frequency range. An equivalent circuit fit at center position ($750\,\mu m$) with

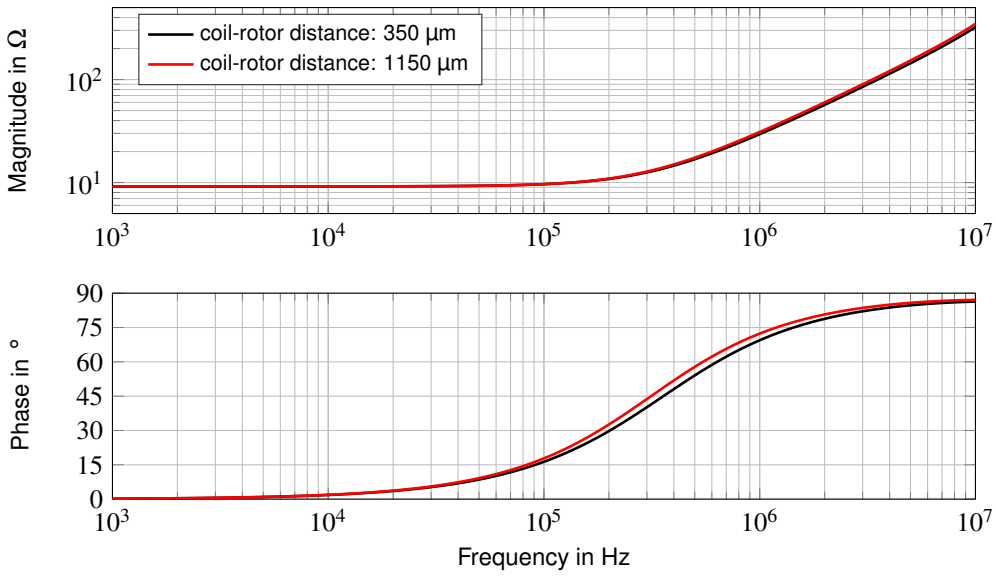

Figure 3: Sensor coil impedance for the boundaries of the nominal operation range (non-shielded design).

$R_{coil} = 9.17\,\Omega$ and $L_{coil} = 4.61\,\mu H$ results in a model magnitude error less than $1\,\%$ for frequencies smaller than $2\,MHz$. For the selection of the sensor operating frequency $f_{carrier}$ the frequency-dependent sensor sensitivity ζ was considered

$$\zeta(f) = \frac{\|Z_{1150\,\mu m}(f) - Z_{350\,\mu m}(f)\|_2}{0.5 \cdot \left(\|Z_{1150\,\mu m}(f)\|_2 + \|Z_{350\,\mu m}(f)\|_2\right)} \tag{2}$$

and is calculated by the impedance values at the boundaries of the nominal operational range. Figure 4 shows the sensor sensitivity as a function of the carrier frequency. It can be seen that the sensitivity is not significant below $40\,kHz$. The gradient of the sensitivity is very high at about $300\,kHz$, flattens at about $2\,MHz$ and increases again for frequencies greater than $3\,MHz$. The carrier frequency was chosen as $1\,MHz$, which results in $5.2\,\%$ sensitivity. If a higher carrier frequency is desired, special care must be taken to parasitic winding capacitances

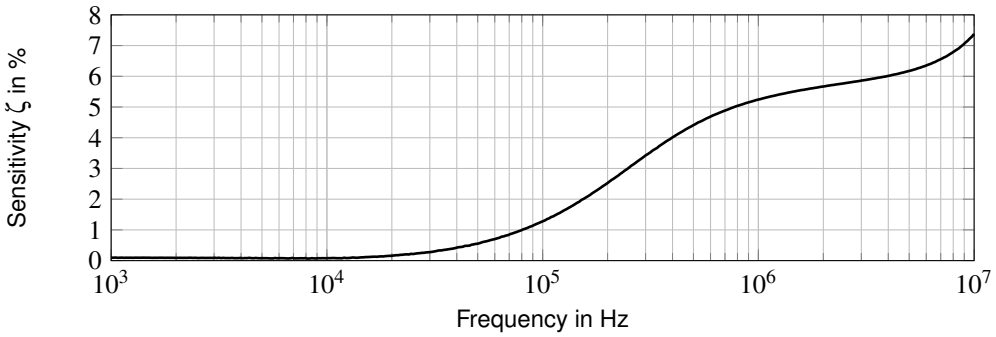

Figure 4: Sensor impedance sensitivity as a function of the carrier frequency (non-shielded design).

concerning PCB manufacturing tolerances and reproducibility. Figure 5 shows the coil characteristic at $1\,MHz$ carrier frequency. It can be seen that the eddy currents in the target material cause a reduction of the impedance magnitude if the rotor is located closer to the sense coil. The overall low value of the impedance magnitude is a result of the small number of winding turns and must be considered in the sensor wiring and circuit design.

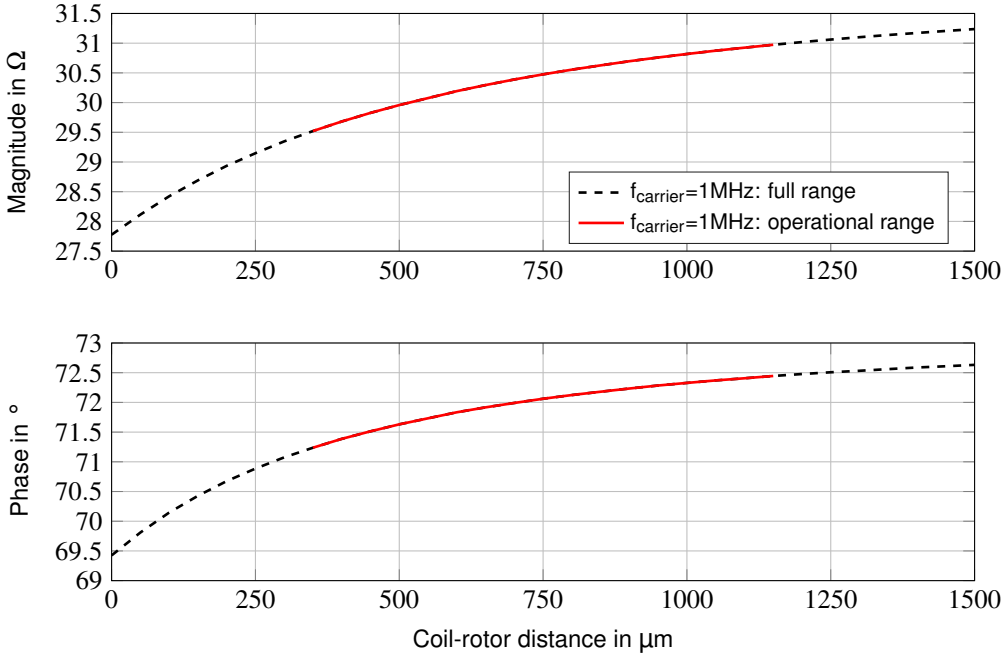

Figure 5: Sensor coil impedance at 1 MHz carrier frequency (non-shielded design).

5. Sensor Circuit and Performance Evaluation

Figure 6 shows an illustration of the electrical circuit for obtaining an output signal which is proportional to the rotor displacement. Two opposing sense coils are connected in a bridge configuration and are excited by a sinusoidal carrier waveform. The differential voltage of the bridge is amplified, band-pass filtered and demodulated to gain the displacement signal. Finally, the signal is low-pass filtered to suppress remaining

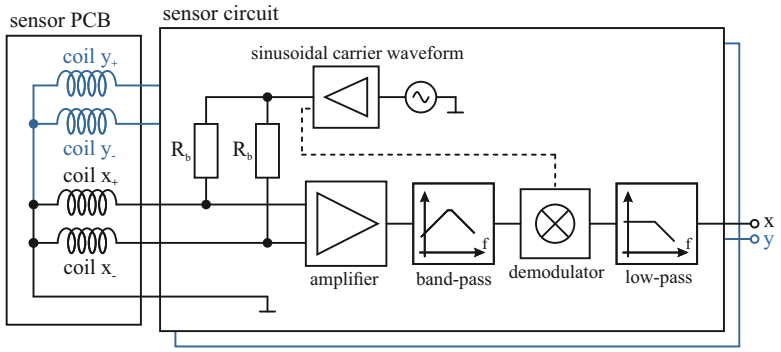

Figure 6: Sensor circuit with sinusoidal carrier waveform excitation and synchronous demodulation.

harmonics of the carrier frequency. Figure 7 and 8 show the output voltage of the sensor circuit for admissible rotor position setpoints as well as the linearity error and noise level, respectively. The non-shielded sensor design features a slightly lower linearity error. Although the shielded design has a lower sensitivity (Fig. 7), the noise

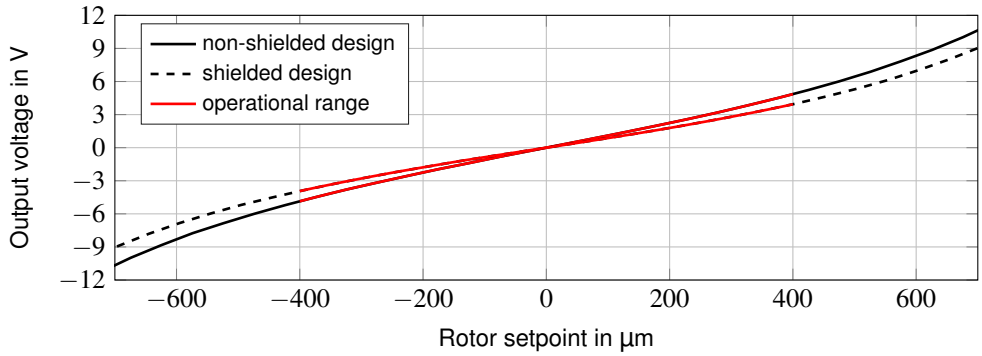

Figure 7: Sensor circuit output voltage as a function of the rotor position setpoint.

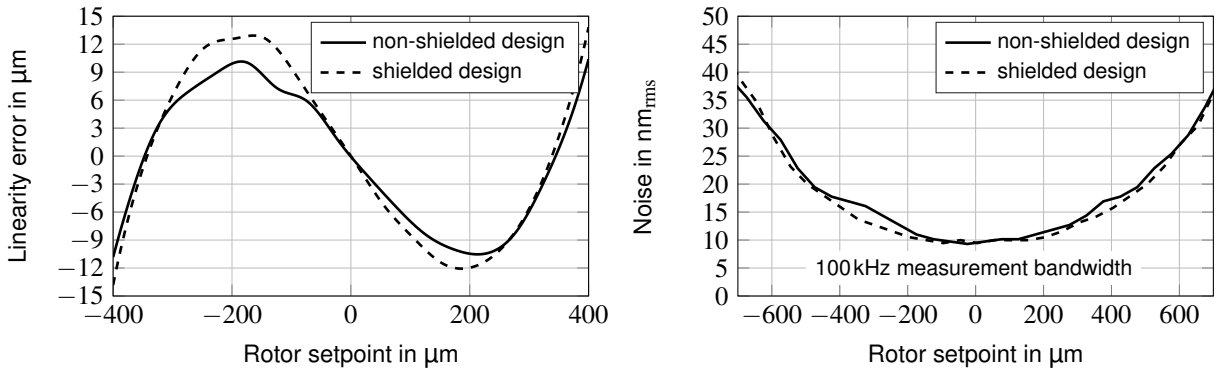

Figure 8: Linearity error and noise as a function of the rotor position setpoint (sensor + sensor circuit).

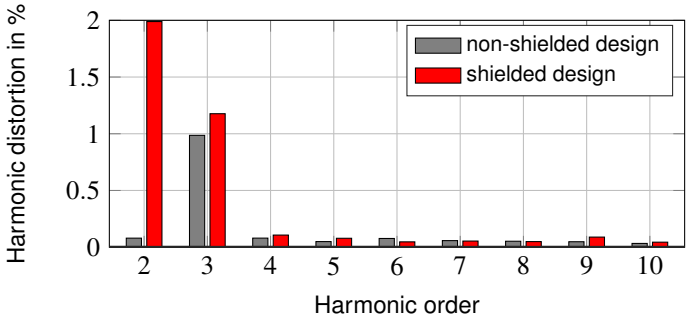

Figure 9: Harmonic distortions of a circular rotor trajectory with 662 µm diameter.

level of the designs is very similar to each other. For obtaining the sensor distortions for circular rotor trajectories, the rotor was $331\,\mu$m eccentrically mounted on a rotary table and was moved along a circular trajectory (Fig. 9).

6. Conclusion

This study covers the design and experimental verification of a PCB integrated eddy current sensor for radial position measurement. A major design objective was to achieve a sensor design with low axial dimension to enable the usage in AMB designs with limitations to the rotor length. The sensor design features an optional shield of the sense coils for the usage in high EMI environments or to suppress the influence of close-by conductive or ferromagnetic elements. Concerning applications with a high spatial temperature gradient, the sensor shield also enables a strong thermal coupling of the sense coils and avoids varying sense coil temperatures, which may lead to undesired signal drifts. Regarding sensor performance, the non-shielded as well as the shielded design obtains a linearity error below $15\,\mu$m and a noise level smaller than $20\,\mathrm{nm_{rms}}$ within the operational range of $\pm 400\,\mu$m rotor displacement. Although the shielded design has a smaller sensitivity, no degradations concerning sensor noise could be detected. Furthermore, a harmonic distortion analysis was performed for circular rotor trajectories which indicated low distortions. Summarized, both sensor designs showed a very good overall performance and seem to be suitable candidates for AMB applications. For future designs, it would be conceivable to integrate the sensor coils and the shield cage in a multilayer PCB design with a higher layer count.

References

Grobler, A. J., van Schoor, G. & Ranft, E. O. (2017), 'Design and optimisation of a pcb eddy current displacement sensor', *SAIEE Africa Research Journal* **108**(1).

Larsonneur, R. & Bühler, P. (2004), 'New radial sensor for active magnetic bearings', *ISMB9, 9th International Symposium on Magnetic Bearings, Lexington, Kentucky, August 3-6* .

Markovic, M. & Perriard, Y. (2009), 'Eddy current power losses in a toroidal laminated core with rectangular cross section', *International Conference on Electrical Machines and Systems, Tokyo, Japan, November 15-18* .

Maslen, E. H. (2006), 'Self–sensing for active magnetic bearings: overview and status', *ISMB10, 10th International Symposium on Magnetic Bearings, Martigny, Switzerland, August 21-23* .

Štusák, M. (2014), 'Eddy current sensors for magnetic bearings of the textile spinning machines', *ISMB14, 14th International Symposium on Magnetic Bearings, Linz, Austria, August 11-14* .

Wang, K., Zhang, L., Zheng, S., Zhou, J. & Liu, X. (2018), 'Analysis and experiment of self-differential eddy-current sensor for high-speed magnetic suspension electric machine', *IEEE Transactions on Industry Applications* **55**(3).